Scleral Crosslinking Using Genipin Can Compromise Retinal Structure and Function in Tree Shrews

Mustapha El Hamdaoui[a], **Alexander M. Levy**[b], **Aaron B. Stuber**[a], **Christopher A. Girkin**[a], **Timothy W. Kraft**[c], **Brian C. Samuels**[a], **Rafael Grytz**[a,*]

[a]Department of Ophthalmology and Visual Sciences, University of Alabama at Birmingham, Birmingham, AL, USA

[b]Department of Biomedical Engineering, University of Alabama at Birmingham, Birmingham, AL, USA

[c]Department of Optometry and Vision Science, University of Alabama at Birmingham, Birmingham, AL, USA

Abstract

Scleral crosslinking using genipin has been identified as a promising treatment approach for myopia control. The efficacy of genipin to alter biomechanical properties of the sclera has been shown in several animal models of myopia but its safety profile remains unclear. In this safety study, we aim to investigate the effect of scleral crosslinking using retrobulbar injections of genipin on retinal structure and function at genipin doses that were shown to be effective in slowing myopia progression in juvenile tree shrews. To this end, three or five retrobulbar injections of genipin at 0 mM (sham), 10 mM, or 20 mM were performed in one eye every other day. Form deprivation myopia was induced in the injected eye. We evaluated retinal function using full-field electroretinography and retinal structure using *in vivo* optical coherence tomography imaging and *ex vivo* histology. The optical coherence tomography results revealed significant thinning of the peripapillary retinal nerve fiber layer in all genipin treated groups including the lowest dose group, which showed no significant treatment effect in slowing myopia progression. In contrast, inducing form deprivation myopia alone and in combination with sham injections caused no obvious thinning of the retinal nerve fiber layer. Electroretinography results showed a significant desensitizing shift of the b-wave semi-saturation constant in the sham group and the second highest genipin dose group, and a significant reduction in b-wave maxima in the two highest genipin dose groups. The *ex vivo* histology revealed noticeable degeneration of photoreceptors and retinal pigment epithelium in one of two investigated eyes of the highest genipin dose group. While scleral crosslinking using genipin may still be a feasible treatment option for myopia control, our results suggest that repeated retrobulbar injections of genipin at 10 mM or higher are not safe in tree shrews. An adequate and sustained delivery strategy of genipin at lower concentrations will be needed to achieve a safe and effective scleral crosslinking treatment

---

*corresponding author: rafaelgrytz@uabmc.edu (Rafael Grytz).

for myopia control in tree shrews. Caution should be taken if the proposed treatment approach is translated to humans.

Keywords

Myopia; Scleral crosslinking; Genipin; Electroretinography; Optical Coherence Tomography

1. Introduction

Myopia is the most common refractive disorder and it is often characterized by an excessive expansion of the scleral shell resulting in an eye with axial length too long relative to its refractive power. With an increasing prevalence worldwide Dolgin (2015); Holden et al. (2016); Morgan et al. (2018) and associated risk for pathological complications Flitcroft (2012); Pan et al. (2012), myopia is a growing global health concern in need of immediate attention. While myopic refractive error can be corrected by wearing glasses or contact lenses, the risk factors for pathological complications associated with myopia, in particular, those associated with high myopia Flitcroft (2012); Pan et al. (2012) cannot be eliminated with such refractive corrections. The currently available non-surgical treatment options for myopia control and management are either partially effective or associated with significant adverse effects Gwiazda (2009); McBrien et al. (2008). The World Health Organization has classified myopia as a worldwide epidemic Flanagan et al. (2019) with an increasing prevalence that is expected to hit nearly 5 billion by 2050 with 1 billion people having high myopia Holden et al. (2016). Thus, the development of effective and safe treatments for myopia control is critical to halt the myopia epidemic.

Myopic eyes are characterized by scleral extracellular matrix remodeling that leads to biomechanical weakening of the sclera, which is thought to be caused by collagen sliding Grytz and El Hamdaoui (2017). Scleral crosslinking (SXL) has been proposed as a novel and promising therapeutic approach to inhibit such remodeling in order to control myopia development and progression in animal models El Hamdaoui et al. (2021); Wang and Corpuz (2015); Wollensak and Iomdina (2008a); Wollensak et al. (2005). SXL for myopia treatment purposes typically involves the administration of a chemical, enzymatic or light-activated crosslinking agent into the subTenon's or retrobulbar space. These agents cause the formation of artificial crosslinks that are thought to stiffen the sclera and prevent sliding between its collagenous components Bailey et al. (1980); Levy et al. (2018); Wollensak and Iomdina (2008b); Wollensak and Spoerl (2004).

Genipin is a natural crosslink agent derived from the geniposide extract of the *Gardenia jasminoides* plant Lee et al. (2003); Ramos-de-la-Peña et al. (2015). The interest for genipin in biomedical, tissue engineering, and clinical applications including SXL has increased in the past years due to its low cytotoxicity, excellent biocompatibility, and effective stiffening characteristics Campbell et al. (2017); Chang et al. (2002); El Hamdaoui et al. (2021); Hannon et al. (2019); Keong and Halim (2009); Lai (2012); Lai et al. (2010); Mi et al. (2002); Sung et al. (1999, 1998); VandeVord et al. (2002); Wang and Corpuz (2015). Several studies have used genipin to alter the mechanical properties of the sclera showing that

genipin can induce sustained scleral stiffening Campbell et al. (2017); Hannon et al. (2019); Liu and Wang (2017), to thicken scleral collagen fibrils Wang and Corpuz (2015), and to reverse biomechanical weakening seen in myopic scleras Levy et al. (2018). *Ex vivo* incubation of scleral tissues in genipin was found to reverse scleral expression of collagen alpha1 chain of type I, matrix metalloproteinase 2, and miR-29 cluster that were found in form deprivation (FD) myopia in guinea pigs Wang et al. (2020). SXL using retrobulbar injections of genipin were found to be effective in slowing FD myopia in guinea pigs Wang and Corpuz (2015) and tree shrews El Hamdaoui et al. (2021), where the treatment effect was found to be dose-dependent. However, only a limited number of studies have investigated potential adverse and toxic effects of using genipin for SXL Hannon et al. (2020); Liu and Wang (2017); Wang and Corpuz (2015). Using histology, no structural damage was identified in the retina, choroid or sclera after four retrobulbar injections of genipin in guinea pig Wang and Corpuz (2015) and rabbit eyes Liu and Wang (2017). In a recent safety study, Hannon et al. (2020) reported that a single retrobulbar injection (150 μl) of genipin at 15 mM did not appear to cause any sustained changes in visual or retinal function, but a slight reduction in retinal ganglion cell axon count. However, the genipin doses of this safety study were significantly lower compared to doses that were found to be effective for myopia control El Hamdaoui et al. (2021); Wang and Corpuz (2015). Moreover, no existing safety study has investigated the adverse effects of genipin at multiple doses. Despite the valuable insights provided in these studies Hannon et al. (2020); Liu and Wang (2017); Wang and Corpuz (2015), the answer to whether genipin-based SXL can be a safe treatment option for myopia control remains inconclusive and more research to that end is warranted.

The goal of this study was to investigate the safety of SXL using genipin at multiple doses including doses that were found effective for myopia control in a translational animal model. To this end, we systemically evaluated the effect of genipin-based SXL on: retinal structure using (i) *in vivo* optical coherence tomography (OCT) and (ii) *ex vivo* histology, and (iii) retinal function using *in vivo* electroretinography (ERG) in tree shrew eyes.

2. Methods

2.1. Experimental Subjects and Groups

Maternally reared juvenile northern tree shrews (*Tupaia glis belangeri*), housed in individual cages on a 14-hour light/10-hour dark cycle with continuous access to food and water McBrien and Norton (1992), were the experimental subjects in this study. Thirty tree shrews were randomly assigned to one of six different experimental groups that differed in (i) visual experience (normal or FD), (ii) retrobulbar injection using genipin or buffer (sham), (iii) genipin concentrations of 10 mM or 20 mM, and (iv) 3 or 5 retrobulbar injections. The experimental groups and their naming conventions are summarized in Table 1. We used monocular FD to induce progressive myopia by fitting the tree shrew with a lightweight aluminum goggle frame with a translucent diffuser in one eye Norton et al. (2003); Ward et al. (2016). Retrobulbar injections of buffer or genipin solution were delivered to the FD eye. The contralateral, non-injected eye served as control. Experimental groups were balanced to include males and females, and no experimental group included pups from the

same parents. Biometry and refractive results of the experimental cohort used in the current study were reported in a previous publication showing the efficacy of genipin-induced SXL on slowing progressive myopia El Hamdaoui et al. (2021). All procedures adhered to the ARVO Statement for the Use of Animals in Ophthalmic and Vision Research and were also approved by the University of Alabama at Birmingham Institutional Animal Care and Use Committee.

2.2. Retrobulbar Injections

Animals were prepared for injections by delivering isoflurane anesthesia (3% in 100% oxygen at 1 l/min) through a nose cone. A sterile field around the skin of the eye was created using 5% povidone iodine washes ×3 and then rinsed with sterile phosphate buffer saline. Topical proparacaine hydrochloride ophthalmic solution (0.5%; Sandoz; Holzkirchen, Germany) was used for additional anesthetic purposes. A traction suture (Ethicon Perma-Hand 7/0, 18" Silk Black, Braided) was placed through the conjunctiva inferior to supraduct the eye. The fornix incision was created in the inferonasal conjunctiva using sharp curved vannas scissors (World Precision Instruments) and dissection carried down through Tenon's capsule keeping the size of the incision minimal. Using tying forceps, the conjunctiva and Tenon's were dissected bluntly so that the muscle cone could be visualized. The muscle tunic was opened near the scleral insertion using the tying forceps to bluntly dissect the tissue. This allowed the visualization of the intraconal fat and posterior pole of the sclera. A 25 gauge blunt curved needle attached to a thin 1 ml insulin syringe was inserted into the retrobulbar space adjacent to the posterior pole sclera and the conjunctiva held and closed tightly around the needle. The syringe was used to deliver genipin or buffer (sham) solution into the retrobulbar space at the posterior pole region at a volume and rate of 400 μl over 15 minutes. The estimated total volume needed to fil the entire retrobulbar space in tree shrew eyes is approximately 75 μl. The initial 75 μl of injectate going into the retrobulbar spaces causes a noticeable bulging of the conjunctiva before the solution begins to gradually leak out of the conjunctival incision and exposes the cornea. The solution, even with some egress out of the conjunctiva, filled the entire retrobulbar space exposing the entire sclera including the posterior pole to the solution.

A genipin stock solution of 50 mg/ml was prepared by dissolving genipin powder (Wako Chemicals USA, Inc, Fisher Scientific) in dimethyl sulfoxide (DMSO; Corning Dimethyl Sulfoxide, Fisher Scientific) to ensure maximum solubility of genipin. The stock solution was aliquoted into small volumes and stored at −25 °C until used. The frozen aliquots were thawed then diluted to the required genipin concentration using an ophthalmic balanced salt solution (BSS; BSS ophthalmic irrigating solution, Alcon) with pH = 7.4 and osmolality of 300 $mOsm/Kg$ before each injection. To ensure that our injections have similar osmolality values, the final injected solutions (genipin and buffer) were adjusted to contain 10% DMSO. Genipin at the concentrations used in the current study has a minuscule impact on osmolality values of the injected solutions of genipin. Although we did not measure the pH of the final injected solutions due to their small volumes, DMSO and genipin are not expected to significantly alter the pH of our buffer BSS (pH = 7.4). DMSO is an aprotic molecule and has no impact on pH values. Genipin has a limited impact on pH values as

genipin's main functional groups are alcohols which have an acid ionization constant similar to that of water.

Each injected group received retrobulbar injections of either buffer (sham) or genipin at different concentrations and number of injections as described in Table 1. Injections were performed every other day starting at 18 days of visual experience (DVE) until the established number of injections for each group was reached as illustrated in Figure 1. Injected eyes were randomly selected and were exposed to a total of 11 days of FD starting at 24 DVE and ending at 35 DVE. The surgeon was blinded to the injectate used for each injection.

The animals were examined daily for potential signs of discomfort, sickness, pain, retinal damage, corneal damage, inflammation, gaze problems, eye movement and scar tissue formation at the site of injection. However, none of these complications was detected in any of our experimental subjects. The conjunctival and muscle incisions were inspected by the surgeon before each injection and no signs of inflammation or scar tissue formation were detected. Although the conjunctival and muscle incisions were left open after performing injections, they both closed up within 48 hours post injection and had to be reopened using blunt dissection for subsequent injections. Upon enucleation, eyes were further inspected, and no apparent differences were found among normal, control and treated eyes. The conjunctival and muscle incisions were found to be closed up and healed with no signs of scar tissue formation.

2.3. Refractive and Biometry Measurements

To evaluate treatment efficacy on developing myopia, refractive error measurements were performed daily from 18 to 35 DVE in fully awake animals using the Nidek ARK-700A infrared auto-refractor (Marco Ophthalmic, Jacksonville, FL) and analyzed following previously established protocols Norton et al. (2010, 2003). Biometry measurements were also performed daily from 18 to 35 DVE in fully awake animals to measure axial eye dimensions using the Lenstar LS-900 optical biometer (Haag-Streit USA, Mason, OH). The Lenstar raw data was analyzed using species- and device-specific refractive indices El Hamdaoui et al. (2019). The refractive and biometry data was previously published in El Hamdaoui et al. (2021) with slightly larger sample sizes. To objectively compare adverse effects with treatment effects, we replotted the refractive and biometry data only for experimental subjects used in the current study.

2.4. Optical Coherence Tomography Imaging

At 34 DVE, OCT scans were performed to assess the effect of the proposed treatment on the peripapillary retinal thickness *in vivo*. Prior to OCT imaging, animals were anesthetized using a 0.02 cc intra-muscular injection of xylazine (100 mg/mL). Hard contact lenses were placed onto the corneas to provide a stable ocular surface for imaging. Isoflurane (1% in 100% oxygen at 1 l/min) was administered through a nose cone attached to a custom built imaging platform with a heating pad to maintain a stable animal position and a constant body temperature at 37 °C throughout the imaging session. A total of 48 radial OCT scans centered on the optic nerve head (ONH) were acquired using the spectral

domain OCT system Spectralis OCT2 (Heidelberg Engineering, Heidelberg, Germany). The acquired OCT radial scans were automatically delineated using the deep learning algorithm Reflectivity (ABYSS Processing; Singapore). Figure 2B shows a representative OCT B-scan with segmented tissue interfaces. The retinal segmentation was divided into two layers: the retinal nerve fiber layer (RNFL) and the remaining retinal layers (RRL). The also segmented sclera, retinal pigment epithelium-choroid complex and lamina cribrosa were not investigated in this study. All delineations were visually inspected to ensure their accuracy.

Small changes in the camera position were previously shown to induce large, nonlinear optical distortions in OCT images of the posterior segment in tree shrew eyes Fuchs et al. (2019). We used our empirical approach Grytz et al. (2022) for nonlinear optical distortion correction to correct these distortions. Figure 3A (top) shows the same B-scan plotted in Figure 2B after nonlinear distortion corrections. Figure 3B shows a 3D reconstruction of all segmented and distortion corrected tissue interfaces of one representative OCT scan consisting of 48 radial B-scans. RNFL and RRL thicknesses were obtained from the 3D reconstruction of their segmented interfaces (Figure 3B) and averaged over a $50\mu m$ thick circular band centered on the anterior scleral canal opening (ASCO) centroid with an inner radius of $750\mu m$ as illustrated in Figures 2A and 3A. Thickness measurements were evaluated along the normal direction of an ellipse that was fitted to the anterior scleral interface.

2.5. Electroretinography (ERG)

As our retrobulbar injections exposed the entire sclera to genipin, we used full-field ERG instead of localized ERG measurements to assess potential adverse effects of genipin on retinal function across the entire retina. ERG measurements were performed at the endpoint of the experiment (35 DVE) using a custom-built ERG system for small animals and in accordance with previously established protocols Clark and Kraft (2012). Briefly, animals were dark adapted for 1 hour prior to the ERG recordings. During the recording, animals were placed in a Faraday cage with the head restrained using a magnetic stand with an alligator clip. Isoflurane was administered through a nose cone (3% in 100% oxygen at 1 L/min) and body temperature was maintained at 37° using a heating pad throughout the entire procedure. Both corneas were treated with 0.5% proparacaine followed by a mixture of 2.5% phenylephrine and 1% tropicamide for pupil dilation. Hard contact lenses with attached gold wired electrodes were put on both eyes to simultaneously record the ERG signal of both eyes. To ensure electric conductivity, a topical conductive agent (2.5% hypromellose ophthalmic demulcent solution, Akorn Pharmaceuticals, Forest Lake, IL, USA) was used as a coupling agent between electrodes and corneas. A tapered silver electrode was clipped onto the right ear to electrically ground the animal. A 100 W tungsten-halogen lamp acted as a light source. A series of 11 neutral density filters with a neutral density value ranging from 0 to 3 were used to control the stimulus intensity delivered to both eyes via fiber-optic cables aligned with a beam-splitter. The wavelength of the light stimulus was 505 nm (35 nm bandwidth). The eyes were stimulated for 10 ms with the light stimulus then a series of sweeps (1000 ms per sweep) was recorded for each neutral density filter. Dim flash strengths were repeated 20 times, to average out noise, and as the stimulus strength was increased the number of responses averaged was reduced to a minimum of 5. To

maintain a dark-adapted state, the inter-stimulus interval was increased systematically from 2.2 to 15.2 *s.* An additional set of 3 sweeps was recorded using a bright camera flash representing our maximum stimulus (I_{max}) with an inter-stimulus interval of 90 *s.* Baseline adjustments were made by subtracting the mean root squares of the measured signals prior to the light stimulation from each sweep. The corrected sweeps were averaged, and the b-wave amplitude was extracted for each stimulus intensity. The unattenuated stimulus was calibrated daily using an optical power meter (Graseby Optronics, Orlando, FL). The effective emitted power from the ERG system's light source was measured after each experiment with a power meter and used to adjust the effective light stimulus delivered to the eyes. A modified Naka–Rushton model of the form

$$V = V_{sat}\frac{I}{I + I_0} + c, \tag{1}$$

was fitted to the b-wave amplitude and adjusted stimulus intensity values recorded for each eye. The parameters V_{sat}, I_0, and c represent the fitted saturation response amplitude, semi-saturation constant, and background noise, respectively. Figure 4A shows a representative ERG trace containing the a-wave and b-wave of a tree shrew eye. Figure 4B shows a schematic representation of the b-wave amplitude-intensity relationship along with the best fit (Equation 1). Figures 4C and D show representative examples of the b-wave amplitude-intensity relationship of two experimental subjects exposed to normal visual experience (Figure 4C) and FD plus genipin treatment (Figure 4D), respectively.

To evaluate the effect of SXL on the b-wave response, the semi-saturation constant I_0 and saturation response amplitude V_{sat} were extracted from the fitted function. The a-wave response was negligible except for the brightest stimuli, which was expected for a cone dominant retina such as that of the tree shrew. Therefore, a-wave comparisons were made using the experimentally measured maximum response V_{max} at I_{max}.

2.6. Histology

After the completion of ERG recordings, tree shrews were euthanized using an intra-muscular injection of ketamine–xylazine (100 mg/ml–100 mg/ml) into the leg followed by a lethal intraperitoneal injection of xylazine (100 mg/ml). A total of four eyes (n=4); one control (untreated, n=1), one sham (FD + 5 × sham, n=1) and two genipin treated eyes (FD + 5 × 20 mM GEN, n=2) were enucleated and preserved by immersion in fixative (2.5% paraformaldehyde and 1% glutaraldehyde in 0.1M phosphate buffer, pH 7.4), then processed for high-resolution histology using methods adapted from those used for human retinas Curcio et al. (2011). A strip of a full-thickness eye wall containing the ONH and the temporal retina area extending to the ora serrata was dissected. Tissue samples were post-fixed in osmium tannic acid paraphenylenediamine, originally used to preserve extracellular lipids in human eyes and found to impart polychromaticity to toluidine bluestained semi-thin sections. Tissues were dehydrated through ascending concentration of alcohols, embedded in epoxy resin (PolyBed 812, EMS, Hatfield PA), and oriented for sectioning in a superior to inferior direction. From each eye, one section approximately 4 mm long and including the ONH was selected for whole-section scanning using a 60x oil-immersistology of control, sham (FD + 5 × sham) and genipin (FD + 5 × 20 mM GEN) ion objective (numerical

aperture = 1.42) and a robotic microscope stage (Olympus VSI 120, CellSens; Olympus, Center Valley PA).

2.7. Analysis

SXL induced adverse effects were defined as significant changes of the OCT derived retinal thicknesses (RNFL and RRL) and the ERG derived parameters (I_0, V_{sat}, V_{max}). The treatment effect on developing myopia was assessed in terms of refractive error and vitreous chamber depth (VCD) development. Differences between treated and control eyes (Treated - Control) for each group and parameter were computed and used for comparison across groups. The groups normal and FD-alone served as reference groups to which all groups with retrobulbar injections were compared. Independent samples t-tests were used to test for significant differences between the injected groups and reference groups. A mixed design analysis of variance with repeated measures (split plot ANOVA) was used to test for differences in the longitudinal development of refractive error and VCD as previously reported in El Hamdaoui et al. (2021). The statistical analysis was performed using MATLAB and SPSS V25. The significance level was set to 0.05. For a thorough analysis of the refraction and biometry data, we refer the reader to our previously published work El Hamdaoui et al. (2021). Histological sections were evaluated in a masked manner for preservation quality and integrity of retinal layers using FIJI Schindelin et al. (2012) to manipulate images.

3. Results

3.1. Treatment Effect on Refractive Error and VCD

The daily development of refractive error and VCD of all experimental groups is shown in Figure 5. Genipin treated groups exhibited a dose-dependent trend in the treatment effect for both, slowing refractive error progression towards myopia and VCD elongation. Compared to the FD-alone group, the refractive error development was found to be significantly different in the normal, FD+3×20mM GEN and FD+5×20mM GEN groups. The progression of VCD elongation was significantly slowed compared to FD in the normal, FD+5×sham, and FD+5×20mM GEN groups.

3.2. Retinal Thickness Changes

The OCT derived retinal thickness changes in terms of differences between treated and control eyes (Treated - Control), and the *p*-values of the t-tests comparing injected groups to the normal and FD-alone groups are summarized in Figure 6 and Table 2, respectively. Results of the OCT data revealed significant RNFL thinning in all genipin treated groups compared to the FD-alone group. Only the highest genipin dose group showed a significant RNFL thinning compared to the normal group. The normal, sham and FD-alone groups showed no significant differences in RNFL thickness across groups suggesting that the observed RNFL thinning in the genipin treated groups was caused by genipin not FD treatment (Figure 6A). In contrast to RNFL, FD treatment alone and in combination with genipin or sham injections caused a significant thinning of RRL compared to that of the normal group. RRL thinning in the genipin and sham groups was less pronounced but not

significantly different compared to that of the FD-alone group (Figure 6B) suggesting that RRL thinning was primarily caused by axial elongation and not by genipin treatment.

3.3. Electroretinography

Figure 7 shows ERG derived results in terms of differences between treated and control eyes (Treated - Control) for the b-wave semi-saturation constant I_0, the fitted b-wave saturation response V_{sat}, and the experimentally measured a-wave maximum response V_{max} at I_{max}. Table 3 shows the output of the statistical analysis of comparing injected groups to normal and FD-alone groups. While two injected groups (FD+5×sham and FD+3×20mM GEN) showed a significant difference in the b-wave semi-saturation I_0 compared to the normal group, no significant differences were found compared to the FD-alone group. The b-wave saturation response V_{sat} was significantly reduced in the two highest genipin dose groups compared to the FD-alone group and in the FD+3×20mM GEN group compared to the normal group. Although the a-wave maximum response V_{max} was slightly reduced in the two highest genipin dose groups, no significant differences were found across groups.

3.4. Histology

Histologic analysis was performed in 4 eyes and selected results are summarized in Figure 8. An untreated control eye (Figure 8 A–B) and its fellow sham-treated eye (Figure 8 C–D) exhibited thick inner retinal layers and a well-organized outer retina with vertically aligned photoreceptors interleaved with melanosome-containing apical processes of the retinal pigment epithelium (RPE). One eye that received the highest dose of genipin (FD + 5 × 20 mM GEN) showed thinning of the inner retina but still organized outer retina (Figure 8 E–F), although the staining of photoreceptor cell bodies was pale. Another eye also receiving the highest dose of genipin (FD + 5 × 20 Mm GEN) had thinning of the inner retina and noticeable degeneration of photoreceptors and RPE (Figure 8 G–H). The latter was manifest as outer nuclear layer thinning, shortening and absence of outer segments, and reduced volume of pigmented apical processes.

4. Discussion

We have presented a preclinical study that evaluated the safety of SXL using genipin for myopia control in tree shrew eyes. To this end, we evaluated the effect of SXL on retinal structure and function using genipin doses that were shown effective in slowing progressive FD myopia in juvenile tree shrews. We measured functional changes using full-field ERG, and structural changes at the tissue- and micro-level using *in vivo* OCT and *ex vivo* histology, respectively. Our OCT results revealed that retrobulbar injections of genipin can lead to significant thinning of the peripapillary RNFL. This RNFL thinning was observed in all genipin treated groups including the lowest dose group (FD+3×10mM GEN), which showed no significant treatment effect in slowing myopia progression. FD alone and in combination with sham injections caused no obvious thinning of the RNFL. Consequently, the observed thinning of the RNFL in the genipin treated groups is likely a toxic effect caused by genipin injections. In contrast to the RNFL, a significant thinning of the RRL (the retinal thickness without RNFL) was observed in the treated eyes of all groups that received FD treatment. The FD-induced RRL thinning was likely caused by

a passive deformation of the retina as the sclera remodeled and VCD elongated during experimental myopia progression. While not significant, genipin treatment seemed to reduce FD-induced RRL thinning, which may have been caused by slowed scleral remodeling and VCD elongation. It is possible that genipin reached the inner layers of the retina (RNFL) by diffusion through the sclera, choroid, RPE, and outer layers of the retina. However, as SXL caused RNFL but not RRL thinning, one might speculate that our genipin injections have led to a cytotoxic exposure of the retinal ganglion cell axons of the optic nerve within the retrobulbar space, where genipin was injected.

Our ERG results suggest that SXL using genipin can compromise retinal function. The reduced b-wave maxima along with desensitizing shifts of the b-wave semi-saturation constant I_0 are all hallmarks of retinal degeneration. Our histology findings revealed a noticeable degeneration of the photoreceptors and RPE in one of two investigated eyes of the highest genipin dose group. Similar abnormalities were not found in control or sham injected eyes. However, our histological evaluation was not conclusive, qualitive in nature, and based on only 4 eyes. If genipin diffused through the sclera and choroid to the retina, we would have expected more significant cytotoxic effects at the outer retina compared to the RNFL. As no significant thinning of the RRL was observed in OCT, it seems more plausible that the primary cytotoxic exposure occurred at the retrobulbar optic nerve, which may have led to secondary retinal ganglion cell death and RNFL thinning as seen in our OCT results.

Of the existing studies that used genipin for SXL, only a few have addressed its safety and potential adverse effects on the retina. For instance, histological findings revealed that genipin-based SXL did not cause any gross structural changes of ocular tissues in guinea pig Wang and Corpuz (2015) and rabbit Liu and Wang (2017) eyes. Recently, Hannon et al. (2020) reported that genipin-based SXL did not seem to impact the visual and retinal function in rat eyes, but an axonal count analysis revealed that retinal ganglion cell counts were reduced although not significantly in genipin treated eyes. This finding is consistent with the RNFL loss reported in the current study and may confirm our speculation that RNFL loss was caused by axonal damage at the level of the optic nerve. Note that in Hannon et al. (2020), a single retrobulbar injection of genipin at a concentration of 15 mM caused no significant changes in the ERG response (retinal function) but a slight reduction in axonal count. Significantly higher doses and multiple injections of genipin were used in our study to achieve a significant treatment effect for myopia control. Consequently, the more pronounced adverse effects seen here, which included a compromised ERG response in the highest genipin dose groups, are consistent with the findings and lower dose used by Hannon et al. (2020).

Table 4 summarizes the reported adverse effects and genipin doses of existing animal studies that used genipin for SXL showing a dose-dependent increase in adverse effects across these studies. Genipin was also found to exhibit cytotoxic effects in cell culture at a concentration of 0.5 mM Kim et al. (2005, 2014); Wang et al. (2011). This concentration is substantially lower than concentrations used for retrobulbar injections in our study and other *in vivo* studies El Hamdaoui et al. (2021); Hannon et al. (2020); Liu and Wang (2017); Wang and Corpuz (2015). However, a direct comparison between cell culture results and our study is difficult as we have not assessed the genipin concentration at the retina.

In conclusion, our study revealed that SXL using repeated injections of genipin at 10–20 mM had adverse effects on retinal structure and function in the tree shrew model of myopia. Compared to previous preclinical studies Hannon et al. (2020); Liu and Wang (2017); Wang and Corpuz (2015), we have used the highest genipin doses for SXL and experienced the most severe adverse effects reported thus far (Table 4). While SXL in general and SXL using genipin may still be a feasible treatment option for myopia control, our results suggest that repeated retrobulbar injections of genipin at 10mM and higher may not be safe for SXL treatment in tree shrew eyes. However, human eyes may tolerate higher doses of genipin given their thicker nerve sheath and sclera. A new delivery strategy of genipin may be needed to achieve a safe and highly effective SXL treatment for myopia control in the tree shrew pre-clinical myopia model. This goal may be achieved by a sustained delivery of genipin to the sclera at a low and safe concentration. Caution should be taken if the proposed treatment approach is translated to human eyes.

Acknowledgments and Funding

References

Bailey A, Light N, Atkins E, 1980. Chemical cross-linking restrictions on models for the molecular organization of the collagen fibre. Nature 288, 408–410. [PubMed: 7432539]

Campbell IC, Hannon BG, Read AT, Sherwood JM, Schwaner SA, Ethier CR, 2017. Quantification of the efficacy of collagen cross-linking agents to induce stiffening of rat sclera. Journal of The Royal Society Interface 14, 20170014. doi:10.1098/rsif.2017.0014. [PubMed: 28381643]

Chang Y, Tsai CC, Liang HC, Sung HW, 2002. In vivo evaluation of cellular and acellular bovine pericardia fixed with a naturally occurring crosslinking agent (genipin). Biomaterials 23, 2447–2457. doi:10.1016/S0142-9612(01)00379-9. [PubMed: 12033592]

Clark ME, Kraft TW, 2012. Measuring rodent electroretinograms to assess retinal function, in: Wang SZ (Ed.), Retinal Development. Methods in Molecular Biology (Methods and Protocols). Humana Press, Totowa, NJ. Volume 884. chapter 19, pp. 265–276. doi:10.1007/978-1-61779-848-1_19.

Curcio CA, Messinger JD, Sloan KR, Mitra A, McGwin G, Spaide RF, 2011. Human chorioretinal layer thicknesses measured in macula-wide, high-resolution histologic sections. Investigative Ophthalmology & Visual Science 52, 3943–3954. doi:10.1167/iovs.10-6377. [PubMed: 21421869]

Dolgin E, 2015. The myopia boom. Nature 519, 276–278. doi:10.1038/519276a. [PubMed: 25788077]

El Hamdaoui M, Gann DW, Norton TT, Grytz R, 2019. Matching the lenstar optical biometer to A-scan ultrasonography for use in small animal eyes with application to tree shrews. Experimental eye research 180, 250–259. doi:10.1016/j.exer.2018.12.008. [PubMed: 30593786]

El Hamdaoui M, Levy AM, Gaonkar M, Gawne TJ, Girkin CA, Samuels BC, Grytz R, 2021. Effect of scleral crosslinking using multiple doses of genipin on experimental progressive myopia in tree shrews. Translational Vision Science & Technology 10, 1. doi:10.1167/tvst.10.5.1.

Flanagan J, Fricke T, Morjaria P, Yasmin S, 2019. Myopia: a growing epidemic. Community eye health 32, 9. [PubMed: 31409944]

Flitcroft DI, 2012. The complex interactions of retinal, optical and environmental factors in myopia aetiology. Prog Retin Eye Res 31, 622–660. doi:10.1016/j.preteyeres.2012.06.004. [PubMed: 22772022]

Fuchs PA, El Hamdaoui M, Henry JL, Grytz R, Samuels BC, 2019. OCT camera position affects apparent eye morphometry in tree shrews (Tupaia belangeri). Investigative Ophthalmology & Visual Science 60, 208.

Grytz R, El Hamdaoui M, 2017. Multi-scale modeling of vision-guided remodeling and age-dependent growth of the tree shrew sclera during eye development and lens-induced myopia. Journal of Elasticity 129, 171–195.doi:10.1007/s10659-016-9603-4. [PubMed: 28966436]

Grytz R, El Hamdaoui M, Fuchs PA, Fazio MA, McNabb RP, Kuo AN, Girkin CA, Samuels BC, 2022. Nonlinear distortion correction for posterior eye segment optical coherence tomography with application to tree shrews. Biomed. Opt. Express 13, 1070–1086. doi:10.1364/BOE.447595. [PubMed: 35284162]

Gwiazda J, 2009. Treatment options for myopia. Optom Vis Sci 86, 624–628. doi:10.1097/OPX.0b013e3181a6a225. [PubMed: 19390466]

Hannon BG, Luna C, Feola AJ, Ritch MD, Read AT, Stinnett SS, Vo H, Pardue MT, Gonzalez P, Ethier CR, 2020. Assessment of visual and retinal function following in vivo genipin-induced scleral crosslinking. Translational Vision Science & Technology 9, 8. doi:10.1167/tvst.9.10.8.

Hannon BG, Schwaner SA, Boazak EM, Gerberich BG, Winger EJ, Prausnitz MR, Ethier CR, 2019. Sustained scleral stiffening in rats after a single genipin treatment. Journal of The Royal Society Interface 16, 20190427. doi:10.1098/rsif.2019.0427. [PubMed: 31615330]

Holden BA, Fricke TR, Wilson DA, Jong M, Naidoo KS, Sankaridurg P, Wong TY, Naduvilath TJ, Resnikoff S, 2016. Global prevalence of myopia and high myopia and temporal trends from 2000 through 2050. Ophthalmology 123, 1036–1042. doi:10.1016/j.ophtha.2016.01.006. [PubMed: 26875007]

Keong LC, Halim AS, 2009. In vitro models in biocompatibility assessment for biomedical-grade chitosan derivatives in wound management. International journal of molecular sciences 10, 1300–1313. doi:10.3390/ijms10031300. [PubMed: 19399250]

Kim BC, Kim HG, Lee SA, Lim S, Park EH, Kim SJ, Lim CJ, 2005. Genipin-induced apoptosis in hepatoma cells is mediated by reactive oxygen species/c-Jun NH_2-terminal kinase-dependent activation of mitochondrial pathway. Biochemical Pharmacology 70, 1398–1407. doi:10.1016/j.bcp.2005.07.025. [PubMed: 16143311]

Kim M, Takaoka A, Hoang QV, Trokel SL, Paik DC, 2014. Pharmacologic alternatives to riboflavin photochemical corneal cross-linking: A comparison study of cell toxicity thresholds. Investigative Ophthalmology & Visual Science 55, 3247–3257. doi:10.1167/iovs.13-13703. [PubMed: 24722697]

Lai JY, 2012. Biocompatibility of genipin and glutaraldehyde cross-linked chitosan materials in the anterior chamber of the eye. International journal of molecular sciences 13, 10970–10985. doi:10.3390/ijms130910970. [PubMed: 23109832]

Lai JY, Li YT, Wang TP, 2010. In vitro response of retinal pigment epithelial cells exposed to chitosan materials prepared with different cross-linkers. International journal of molecular sciences 11, 5256–5272. doi:10.3390/ijms11125256. [PubMed: 21614206]

Lee S, Lim J, Bhoo S, Paik YS, Hahn TR, 2003. Colorimetric determination of amino acids using genipin from Gardenia jasminoides. Analytica Chimica Acta 480, 267–274. doi:10.1016/S0003-2670(03)00023-0.

Levy AM, Fazio MA, Grytz R, 2018. Experimental myopia increases and scleral crosslinking using genipin inhibits cyclic softening in the tree shrew sclera. Ophthalmic & physiological optics : the journal of the British College of Ophthalmic Opticians (Optometrists) 38, 246–256. doi:10.1111/opo.12454. [PubMed: 29691925]

Liu TX, Wang Z, 2017. Biomechanics of sclera crosslinked using genipin in rabbit. International Journal of Ophthalmology 10, 355–360. doi:10.18240/ijo.2017.03.05. [PubMed: 28393024]

McBrien NA, Norton TT, 1992. The development of experimental myopia and ocular component dimensions in monocularly lid-sutured tree shrews (Tupaia belangeri). Vision Res 32, 843–852. doi:10.1016/0042-6989(92)90027-G. [PubMed: 1604853]

McBrien NA, Young TL, Pang CP, Hammond C, Baird P, Saw SM, Morgan IG, Mutti DO, Rose KA, Wallman J, Gentle A, Wildsoet CF, Gwiazda J, Schmid KL, Smith E, Troilo D, Summers-Rada J, Norton TT, Schaeffel F, Megaw P, Beuerman RW, McFadden SA, 2008. Myopia: Recent advances in molecular studies; prevalence, progression and risk factors; emmetropization; therapies; optical links; peripheral refraction; sclera and ocular growth; signalling cascades; and animal models. Optom Vis Sci 86, 45–66. doi:10.1097/01.opx.0000344146.84135.68.

Mi FL, Tan YC, Liang HF, Sung HW, 2002. In vivo biocompatibility and degradability of a novel injectable-chitosan-based implant. Biomaterials 23, 181–191. doi:10.1016/S0142-9612(01)00094-1. [PubMed: 11762837]

Morgan IG, French AN, Ashby RS, Guo X, Ding X, He M, Rose KA, 2018. The epidemics of myopia: Aetiology and prevention. Progress in retinal and eye research 62, 134–149. doi:10.1016/j.preteyeres.2017.09.004. [PubMed: 28951126]

Norton TT, Amedo AO, Siegwart JT, 2010. The effect of age on compensation for a negative lens and recovery from lens-induced myopia in tree shrews (Tupaia glis belangeri). Vision Res 50, 564–576. doi:10.1016/j.visres.2009.12.014. [PubMed: 20045711]

Norton TT, Wu WW, Siegwart JT Jr, 2003. Refractive state of tree shrew eyes measured with cortical visual evoked potentials. Optom Vis Sci 80, 623–631. doi:10.1097/00006324-200309000-00006. [PubMed: 14502042]

Pan CW, Ramamurthy D, Saw SM, 2012. Worldwide prevalence and risk factors for myopia. Ophthalmic Physiol Opt 32, 3–16. doi:10.1111/j.1475-1313.2011.00884.x. [PubMed: 22150586]

Ramos-de-la-Peña AM, Montañez JC, de la Luz Reyes-Vega M, Hendrickx ME, Contreras-Esquivel JC, 2015. Recovery of genipin from genipap fruit by high pressure processing. LWT - Food Science and Technology 63, 1347–1350. doi:10.1016/j.lwt.2015.04.038.

Schindelin J, Arganda-Carreras I, Frise E, Kaynig V, Longair M, Pietzsch T, Preibisch S, Rueden C, Saalfeld S, Schmid B, et al. , 2012. Fiji: an open-source platform for biological-image analysis. Nature Methods 9, 676–682. doi:10.1038/nmeth.2019. [PubMed: 22743772]

Sung HW, Huang RN, Huang LL, Tsai CC, 1999. In vitro evaluation of cytotoxicity of a naturally occurring cross-linking reagent for biological tissue fixation. Journal of Biomaterials Science, Polymer Edition 10, 63–78. doi:10.1163/156856299X00289. [PubMed: 10091923]

Sung HW, Huang RN, Huang LL, Tsai CC, Chiu CT, 1998. Feasibility study of a natural crosslinking reagent for biological tissue fixation. Journal of Biomedical Materials Research: An Official Journal of The Society for Biomaterials, The Japanese Society for Biomaterials, and the Australian Society for Biomaterials 42, 560–567. doi:10.1002/(SICI)1097-4636(19981215)42:4<560::AID-JBM12>3.0.CO;2-I.

VandeVord PJ, Matthew HW, DeSilva SP, Mayton L, Wu B, Wooley PH, 2002. Evaluation of the biocompatibility of a chitosan scaffold in mice. Journal of Biomedical Materials Research: An Official Journal of The Society for Biomaterials, The Japanese Society for Biomaterials, and The Australian Society for Biomaterials and the Korean Society for Biomaterials 59, 585–590. doi:10.1002/jbm.1270.

Wang C, Lau TT, Loh WL, Su K, Wang DA, 2011. Cytocompatibility study of a natural biomaterial crosslinker–genipin with therapeutic model cells. Journal of Biomedical Materials Research Part B: Applied Biomaterials 97B, 58–65. doi:10.1002/jbm.b.31786.

Wang M, Corpuz CCC, 2015. Effects of scleral cross-linking using genipin on the process of form-deprivation myopia in the guinea pig: a randomized controlled experimental study. BMC Ophthalmol 15, 89. doi:10.1186/s12886-015-0086-z. [PubMed: 26220299]

Wang M, Yang ZK, Liu H, Li R.q., Liu Y, Zhong WJ, 2020. Genipin inhibits the scleral expression of miR-29 and MMP2 and promotes COL1A1 expression in myopic eyes of guinea pigs. Graefe's Archive for Clinical and Experimental Ophthalmology doi:10.1007/s00417-020-04634-7.

Ward AH, Siegwart JT Jr, Frost MR, Norton TT, 2016. The effect of intravitreal injection of vehicle solutions on form deprivation myopia in tree shrews. Experimental eye research 145, 289–296. doi:10.1016/j.exer.2016.01.015. [PubMed: 26836248]

Wollensak G, Iomdina E, 2008a. Crosslinking of scleral collagen in the rabbit using glyceraldehyde. Journal of Cataract & Refractive Surgery 34, 651–656. doi:10.1016/j.jcrs.2007.12.030. [PubMed: 18361989]

Wollensak G, Iomdina E, 2008b. Long-term biomechanical properties after collagen crosslinking of sclera using glyceraldehyde. Acta Ophthalmol 86, 887–893. doi:10.1111/j.1755-3768.2007.01156.x. [PubMed: 18537936]

Wollensak G, Iomdina E, Dittert DD, Salamatina O, Stoltenburg G, 2005. Cross-linking of scleral collagen in the rabbit using riboflavin and UVA. Acta Ophthalmologica Scandinavica 83, 477–482. doi:10.1111/j.1600-0420.2005.00447.x. [PubMed: 16029274]

Wollensak G, Spoerl E, 2004. Collagen crosslinking of human and porcine sclera. J Cataract Refract Surg 30, 689–695. doi:10.1016/j.jcrs.2003.11.032. [PubMed: 15050269]
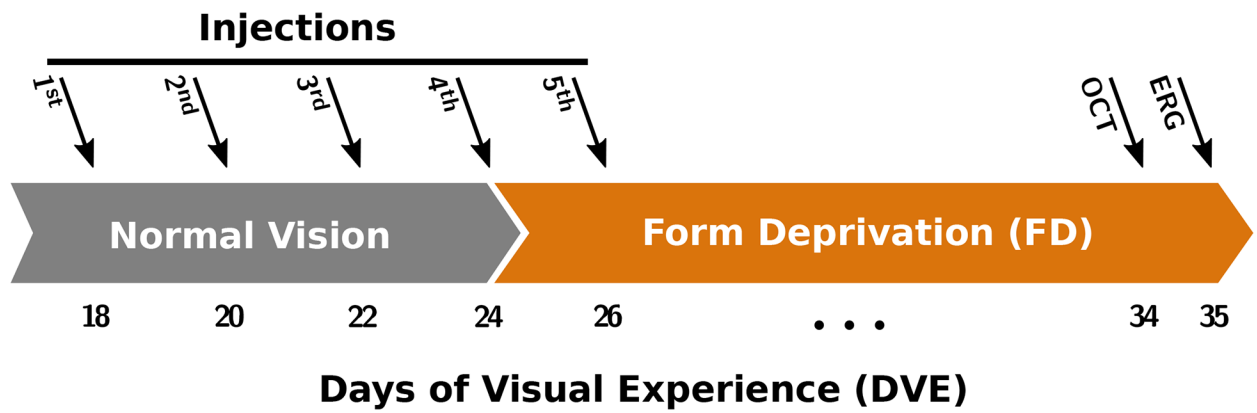
- Repeated retrobulbar injections of genipin at 10mM or higher compromise retinal structure and function in tree shrews

- Scleral crosslinking using genipin at doses that are effective in slowing myopia are not safe in tree shrews

- Caution should be taken if scleral crosslinking using genipin is translated to humans

Injections

1st 2nd 3rd 4th 5th

OCT ERG

Normal Vision

Form Deprivation (FD)

18   20   22   24   26   . . .   34   35

**Days of Visual Experience (DVE)**

Figure 1:

A timeline showing the time and order of each procedure. Retrobulbar injections were performed every other day between 18 and 26 DVE. FD treatment started at 24 DVE and continued until the experimental end point at 35 DVE. Optical coherence tomography (OCT) images were acquired at 34 DVE. Electroretinography (ERG) recordings were performed at 35 DVE, and animals were euthanized immediately afterwards. Refractive error and axial dimensions were measured daily without anesthesia from 18 to 35 DVE.
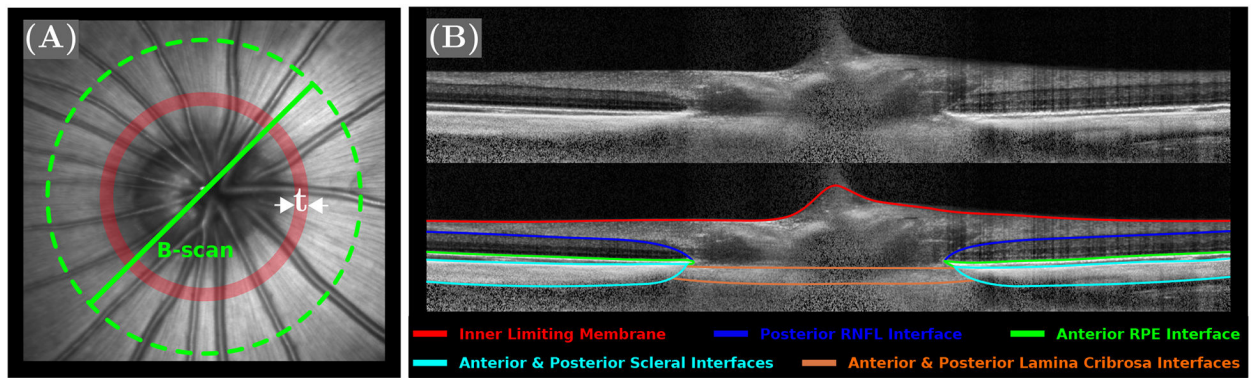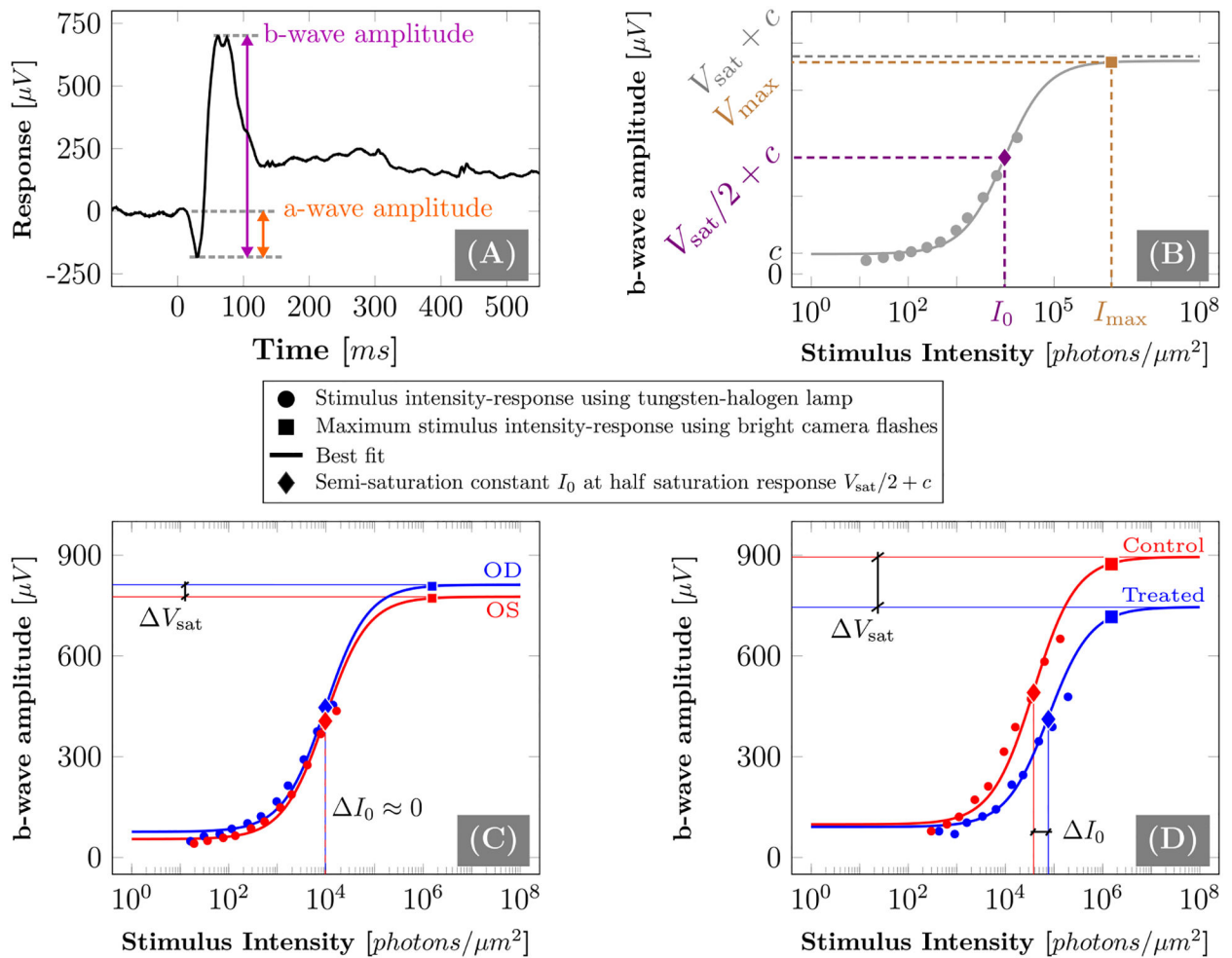
Figure 2:
A: A representative en face image (scanning laser ophthalmoscopy) of the tree shrew ONH. The dashed green line represents the boundaries of the radial B-scans and the red narrow band, with $t = 50\mu m$ represents the area, where retinal nerve fiber layer (RNFL) and remaining retinal layers (RRL) thickness measurements were averaged. **B**: A representative OCT B-scan centered on the tree shrew ONH is shown with (bottom) and without (top) auto-segmented tissue interfaces.
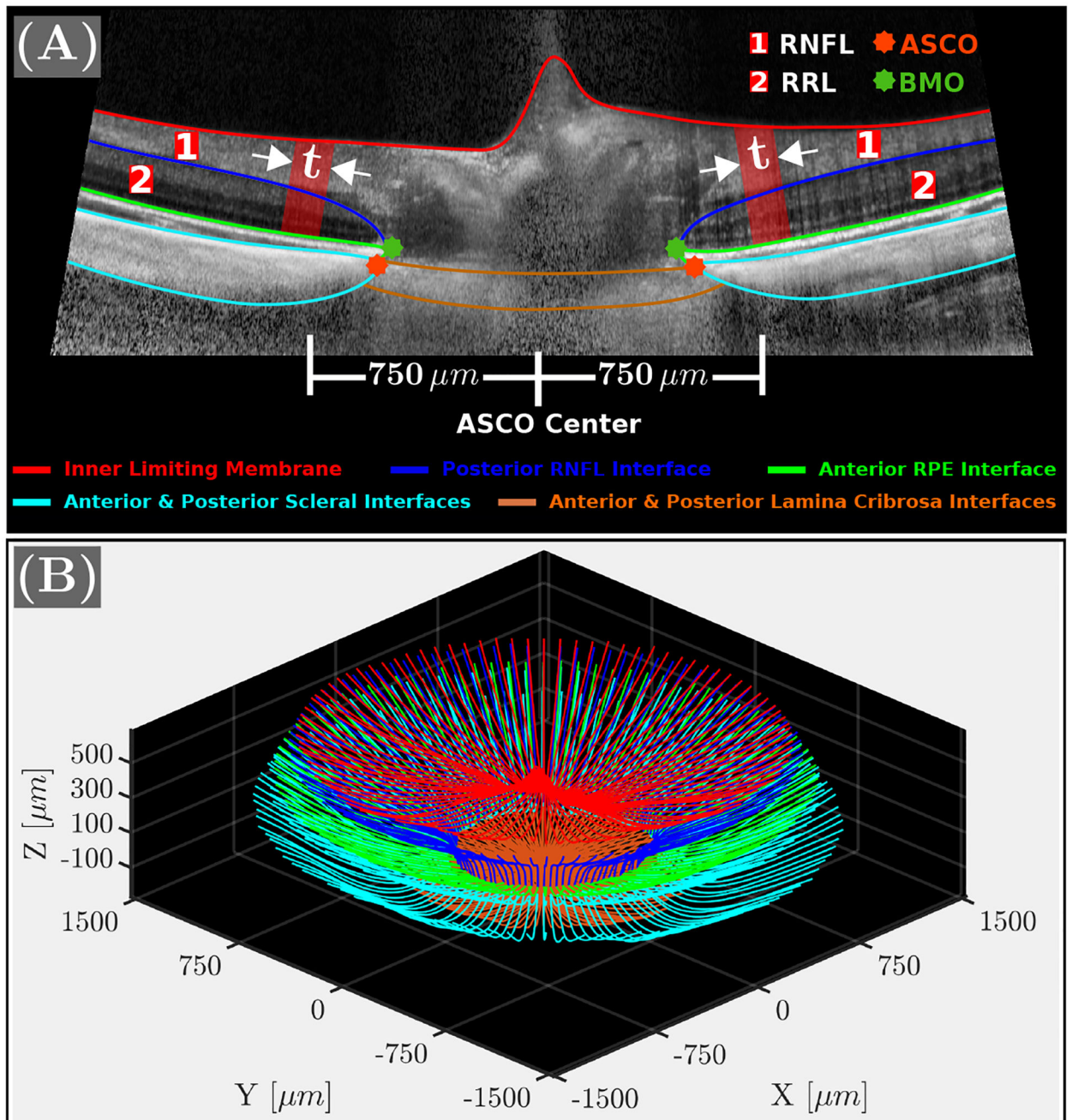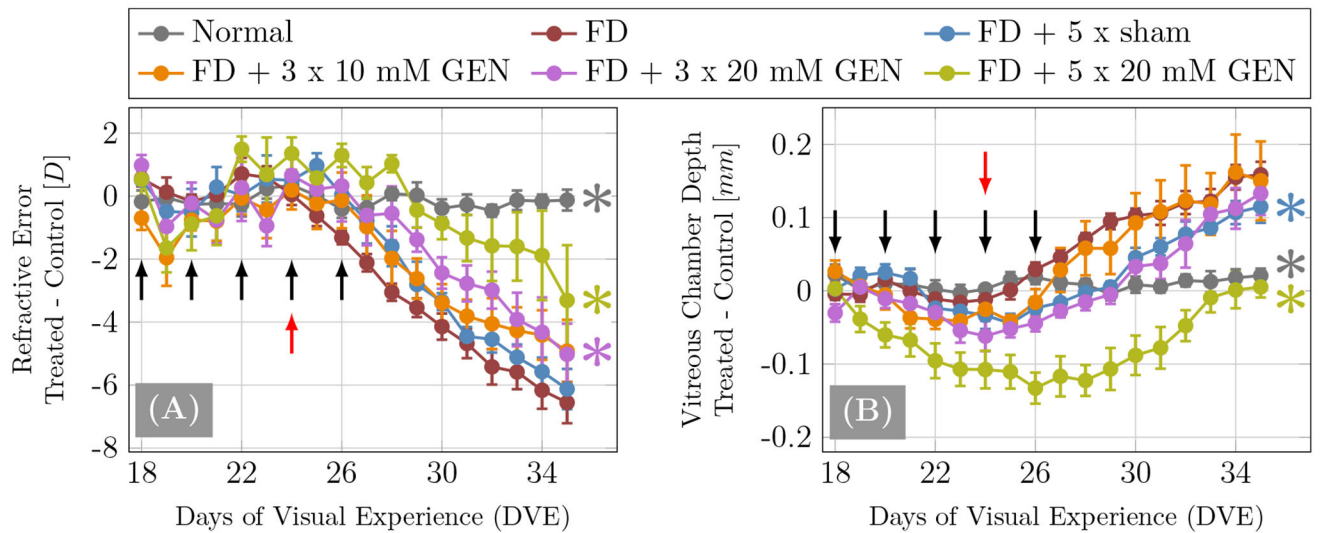
Figure 3:
A: Distortion-corrected OCT B-scan with tissue interfaces. Retinal nerve fiber layer (RNFL) and remaining retinal layers (RRL) thicknesses were averaged across the red band (50μm) located at 750μm from the anterior scleral canal opening (ASCO) center. **B**: 3D reconstruction of the auto-segmented and distortion corrected tissue interfaces of all 48 radial B-scans.
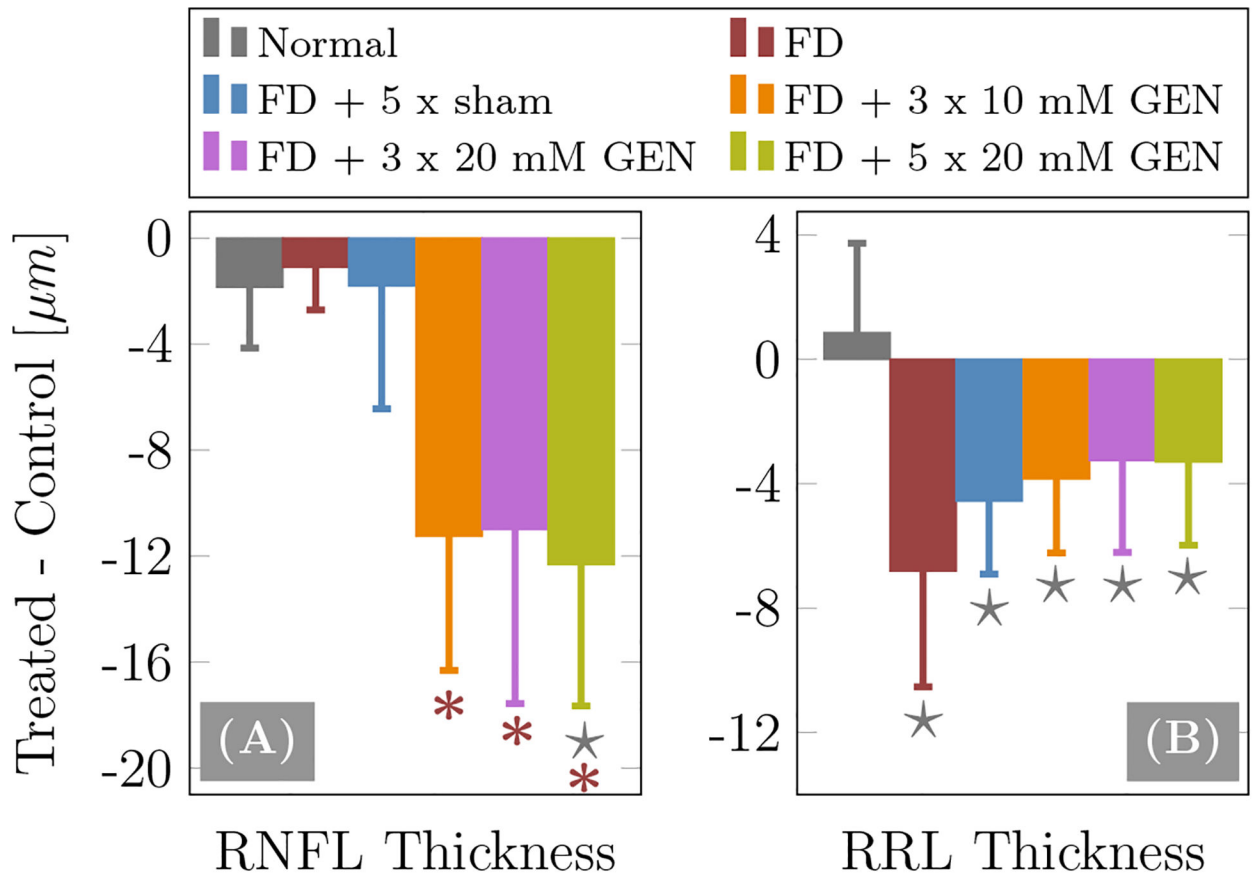
Figure 4:

A: A representative ERG trace of a tree shrew eye showing the a- and b-wave. **B**: An illustration of the intensity-response relationship. Filled circles and squares represent the experimentally measured stimulus-response at different stimulus intensities using the tungsten-halogen lamp and camera flashes, respectively. The solid line represents the best fit of the Naka–Rushton model. Filled diamonds represent the semi-saturation response $V_{sat}/2 + c$ at I_0, where V_{sat} and I_0 represents the fitted saturation response amplitude and semi-saturation stimulus constant, respectively. V_{max} represents the experimentally measured response at the maximum intensity $I_{max}$ that was used during each ERG recording. **C**, **D**: Two representative examples of the b-wave intensity-response relationship data and the fitted Naka–Rushton model (Eq. 1) of a normal (**C**) and genipin treated experimental subject (**D**).

Figure 5:
Plots of daily development of differences between treated and control eye of (**A**) refractive error and (**B**) vitreous chamber depth from 18 to 35 DVE. Black arrows indicate the days on which injections were performed while the red arrow indicates the start of form deprivation (FD) treatment. The groups that showed significant differences ($p < 0.05$, split plot ANOVA) compared to the FD-alone group are marked by a colored asterisk (*) on the right side of each curve.

Figure 6:
OCT results of (**A**) retinal nerve fiber layer (RNFL) thickness and (**B**) remaining retinal layers (RRL) thickness. Shown are differences between treated and control eyes for injected groups or right and left eyes for the normal group. The error bars represent the standard deviation. The ★ and * represent significant group differences ($p < 0.05$) with respect to the normal and FD-alone groups, respectively.
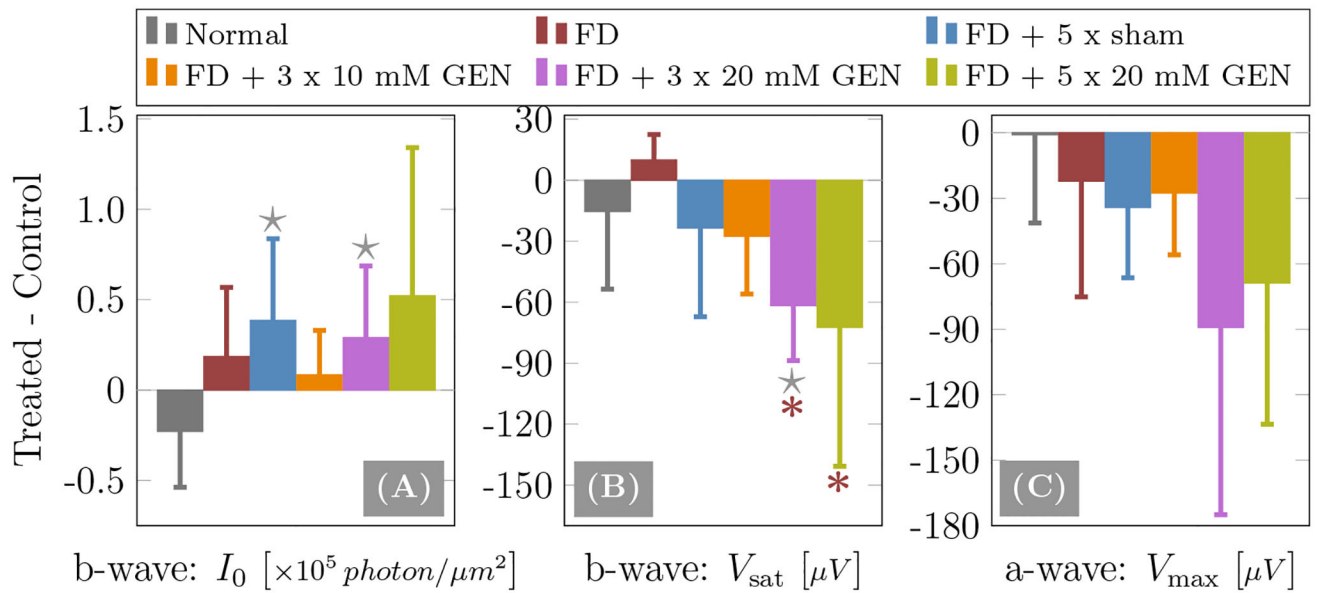
Figure 7:
ERG results of (**A**) b-wave semi-saturation constant I_0, (**B**) b-wave saturation response V_{sat} and (**C**) a-wave maximum response V_{max}. Shown are differences between treated and control eyes for injected groups or right and left eyes for the normal group. The error bars represent the standard deviation. The ⋆ and ∗ represent significant group differences ($p < 0.05$) with respect to the normal and FD-alone groups, respectively.
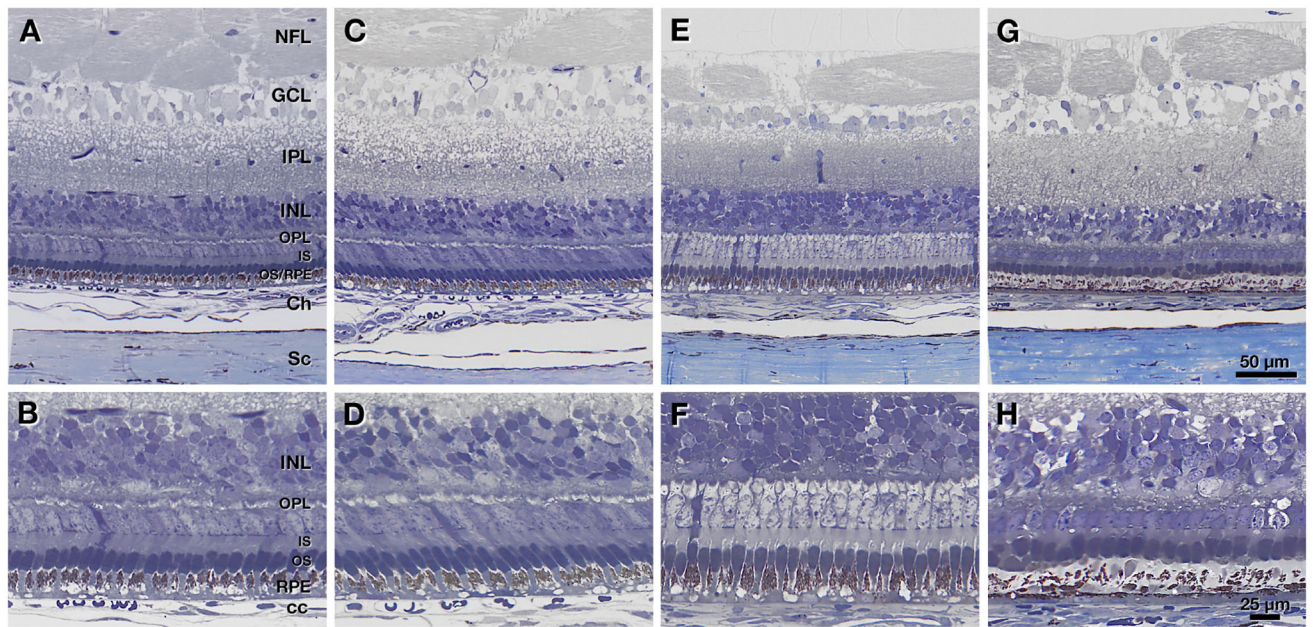
Figure 8:

Histology of control (untreated, n=1), sham treated (FD + 5 × sham, n=1) and genipin treated (FD + 5 × 20 mM GEN, n=2) tree shrew eyes. **A**, **C**, **E**, and **G** show overviews of retina and choroid from the peripapillary region close to the ONH. **B**, **D**, **F**, and **H** show high-magnification views of outer retina at the same locations. The ganglion cell layer (GCL) was poorly preserved and highly vacuolated in all specimens. **A**, **B**: Normal eye has thick inner retinal layers with vertically aligned photoreceptors and apical processes of the retinal pigment epithelium (RPE), the latter recognized by the content of darkly pigmented melanosomes. **C**, **D**: Sham-injected eye also has thick inner retinal layers with organized vertically aligned photoreceptors. **E**, **F**: An eye receiving the highest genipin dose exhibits inner retinal thinning. Photoreceptors are still organized and vertically aligned. Pale staining of photoreceptor cell bodies in the outer nuclear layer could not be definitively attributed to an effect of genipin, an effect of the fixation, or both. **G**, **H**: Another eye receiving the highest dose of genipin exhibits retinal thinning and noticeable degeneration of photoreceptors and RPE, manifest as outer nuclear layer thinning, shortening and absence of outer segments, and reduction in the area of pigmented apical processes. Abbreviations: NFL, nerve fiber layer; GCL, ganglion cell layer; IPL, inner plexiform layer; INL, inner nuclear layer; OPL, outer plexiform layer; IS, inner segments of photoreceptor; OS, outer segments of photoreceptors; RPE, retinal pigment epithelium; Ch, choroid; CC, choriocapillaris; Sc, sclera.

Table 1:

Experimental group names alongside a brief description of the visual experience and treatment received by each group.

Group	Description
Normal	Normal visual experience with no retrobulbar injections (n=5)
FD-alone	FD treatment with no retrobulbar injections (n=5)
FD+5×sham	FD treatment with 5 retrobulbar buffer injections at 0 mM(n=5)
FD+3×10mM GEN	FD treatment with 3 retrobulbar genipin injections at 10 mM (n=5)
FD+3×20mM GEN	FD treatment with 3 retrobulbar genipin injections at 20 mM (n=5)
FD+5×20mM GEN	FD treatment with 5 retrobulbar genipin injections at 20 mM (n=5)

Table 2:

Summary of the statistical analysis output showing the p-values for comparisons of retinal nerve fiber layer (RNFL) and remaining retinal layers (RRL) thicknesses across groups. Statistically significant results ($p < 0.05$) are highlighted in bold font.

	compared to Normal		compared to FD	
	RNFL	**RRL**	**RNFL**	**RRL**
Normal	---	---	0.724	**0.009**
FD	0.724	**0.009**	---	---
FD+5×sham	0.816	**0.012**	0.866	0.255
FD+3×10mM GEN	0.071	**0.021**	**0.008**	0.183
FD+3×20mM GEN	0.074	**0.043**	**0.020**	0.119
FD+5×20mM GEN	**0.034**	**0.041**	**0.006**	0.181

Table 3:

Summary of the statistical analysis output showing the p-values for comparisons of the b-wave semi-saturation constant I_0, b-wave saturation response V_{sat} and a-wave maximum response V_{max} across groups. Statistically significant results ($p < 0.05$) are highlighted in bold font.

	compared to Normal			compared to FD		
	I_0 b-wave	V_{sat} b-wave	V_{max} a-wave	I_0 b-wave	V_{sat} b-wave	V_{max} a-wave
Normal	---	---	---	0.108	0.432	0.096
FD	0.108	0.432	0.096	---	---	---
FD+5×sham	**0.023**	0.946	0.109	0.228	0.409	0.738
FD+3×10mM GEN	0.114	0.582	0.251	0.829	0.135	0.507
FD+3×20mM GEN	**0.041**	**0.043**	0.060	0.463	**0.0004**	0.798
FD+5×20mM GEN	0.087	0.133	0.055	0.333	**0.0498**	0.627

Table 4:

Comparison of reported treatment and adverse effects in animal studies that used genipin for SXL. Listed are the animal model, number of injections (Inj), time interval between injections, concentration (Conc), volume (Vol) of each injection, and the total administered dose of genipin, along with the reported treatment effects and adverse effects.

Study	Model	Inj	Interval	Conc	Vol	Total Dose	Reported Treatment Effects	Reported Adverse Effects
Wang and Corpuz (2015)	Guinea pig	3	7 Days	22 mM	100 μl	1.49 mg	Significant decrease in FD myopia and axial length.	No observed histological damage. Significant thickening of scleral collagen fibrils.
Liu and Wang (2017)	Rabbit	4	2–3 Days	0.5 mM	500 μl	0.22 mg	Significant increase in tissue stiffness.	No observed histological damage.
Hannon et al. (2019, 2020)	Rat	1	-	15 mM	150 μl	0.50 mg	Significant increase in tissue stiffness.	No significant effect on retinal and visual function. Reduced axons in the optic nerve.
El Hamdaoui et al. (2021) and current	Tree shrew	3	2 Days	10 mM	400 μl	2.70 mg	No significant effect on FD myopia and axial elongation.	Significant RNFL thinning and corneal thickening.
		3	2 Days	20 mM	400 μl	5.43 mg	Significant effect on FD myopia but no effect on axial elongation.	Compromised retinal function, significant RNFL thinning and corneal thickening.
		5	2 Days	20 mM	400 μl	9.04 mg	Significant effect on FD myopia and axial elongation.	Compromised retinal function, significant RNFL thinning and corneal thickening.